Journal of Biomolecular Structure & Dynamics, ISSN 0739-1102
Volume 18, Issue Number 1, (2000)

The Identification of Tryptophan Residues Responsible for ATP-Induced Increase in Intrinsic Fluorescence of Myosin Subfragment 1

http://www.adeninepress.com

Ya. K. Reshetnyak[1,2], O. A. Andreev[1,2]*, J. Borejdo[2], D. D. Toptygin[3], L. Brand[3] and E. A. Burstein[1]

[1]Institute of Theoretical and Experimental Biophysics, Russia Academy of Science, 142292 Pushchino, Moscow Region, Russia

[2]Department of Molecular Biology and Immunology, University of North Texas Health Science Center, 3500 Camp Bowie Blvd., Fort Worth, TX 76107, USA

[3]Department of Biology, John Hopkins University, 3400 Charles St., Baltimore, MD 21218

Abstract

ATP binding to myosin subfragment 1 (S1) induces an increase in tryptophan fluorescence. Chymotryptic rabbit skeletal S1 has 5 tryptophan residues (Trp113, 131, 440, 510 and 595), and therefore the identification of tryptophan residues perturbed by ATP is quite complex. To solve this problem we resolved the complex fluorescence spectra into log-normal and decay-associated components, and carried out the structural analysis of the microenvironment of each tryptophan in S1. The decomposition of fluorescence spectra of S1 and S1-ATP complex revealed 3 components with maxima at ca. 318, 331 and 339-342 nm. The comparison of structural parameters of microenvironment of 5 tryptophan residues with the same parameters of single-tryptophan-containing proteins with well identified fluorescence properties applying statistical method of cluster analysis, enabled us to assign Trp595 to 318 nm, Trp440 to 331 nm, and Trp113, 131 and 510 to 342 nm spectral components. ATP induced an almost equal increase in the intensities of the intermediate (331 nm) and long-wavelength (342 nm) components, and a small decrease in the short component (318 nm). The increase in the intermediate component fluorescence most likely results from an immobilization of some quenching groups (Met437, Met441 and/or Arg444) in the environment of Trp440. The increase in the intensity and a blue shift of the long component might be associated with conformational changes in the vicinity of Trp510. However, these conclusions can not be extended directly to the other types of myosins due to the diversity in the tryptophan content and their microenvironments.

Introduction

Muscle contraction results from cyclic interactions of myosin heads with actin filaments driven by ATP hydrolysis. The fundamental question of muscle contraction is how the hydrolysis of ATP is coupled to force generation. The study of tryptophan fluorescence may give the insights to understanding of structural changes produced by ATP in myosin. It has been shown that ATP induced the difference tryptophan absorption (1) and fluorescence excitation (2,3) spectra of myosin. Werber et al. (4) found that ATP induced an enhancement of tryptophan fluorescence of myosin, heavy meromyosin (HMM) and myosin subfragment 1 (S1). The binding of ATP increased the anisotropy of fluorescence of S1, which indicated a decrease of tryptophan mobility in S1 on the nanosecond time scale (5,6). The nucleotide-induced fluorescence enhancement has been exploited to investigate the kinetics of myosin and actomyosin ATPase activity (7-10). Therefore it is important to identify the tryptophans affected by the nucleotides.

Rabbit skeletal myosin S1 has five tryptophan residues (Trp113, 131, 440, 510 and 595), and therefore the identification of fluorophores responsible for the ATP-induced enhancement of fluorescence is quite complex. Torgerson (11) applied the method of decomposition of rabbit skeletal S1 fluorescence spectrum into decay-associated spectral components to resolve the contributions of individual trypto-

*Phone:817-735-2127;
Fax:817-735-2118;
E-mail: oandreev@hsc.unt.ed

phans or groups of tryptophans in the emission of S1 in presence and absence of ATP. Three components associated with fluorescence lifetimes 0.72 (maximum at ca. 320 nm), 4.5 (ca. 330 nm) and 8.8 ns (ca. 345 nm) were revealed by this method. ATP induced an increase in fluorescence intensity of the intermediate and long lifetime associated components by 29% and 9%, respectively, while the shortest lifetime associated component remained unchanged. The chemical modification of Trp131 and Trp113 has no effect on a fluorescence enhancement by ATP (12, 13), and therefore, these tryptophan residues are unlikely to be the ATP-sensitive tryptophans in skeletal S1. It has been suggested that ATP-perturbed tryptophan residue(s) might be close to the segment which includes reactive thiol groups Cys697 and Cys707, because this segment undergoes conformational changes upon ATP binding (14). Based on proximity arguments and fluorescence energy transfer measurements between tryptophans and fluorescent probes attached to Cys697 (15) or Cys707 (16-17) it has been proposed that the Trp510 might be responsible for the fluorescence changes. Recently, Batra and Manstein (18) showed that the replacement of Trp501 by tyrosine residue led to the loss of ATP-induced enhancement of tryptophan fluorescence of *Dictyostelium discoideum* myosin subfragment 1 (Dicty S1). Wild type of Dicty S1 exhibits much less fluorescence enhancement than that by rabbit skeletal S1 (19). Dicty S1 has 4 tryptophan residues, which are in different environment than that of skeletal S1; therefore the effect of ATP on tryptophan fluorescence might be different for these S1s.

In the present work we attempted to identify tryptophan residue(s) that could be responsible for the ATP-induced enhancement of intrinsic fluorescence of rabbit skeletal S1. To solve this problem we applied the methods of the decomposition of protein tryptophan fluorescence spectra into steady-state log-normal components (20-22) and into the decay-associated spectral components (23) in combination with structural analysis of the tryptophan microenvironment (24-27) based on the X-ray structure of S1 (28). The results suggested that Trp440 and Trp510 contributed in ATP-induced increase in intrinsic fluorescence of skeletal S1.

Materials and Methods

Materials

ATP, acrylamide and chymotrypsin were from Sigma (St. Louis, MO).

Preparation of Proteins

Myosin was prepared from rabbit skeletal muscle according to the method of Tonomura et al. (29). S1 was obtained by chymotryptic digestion of myosin and separated into two isoforms by DEAE-cellulose chromatography (30). S1 carrying the essential light chain 1 (LC1) was used in the experiments. The protein concentrations were measured by absorbance at 280 nm, using $A^{1\%} = 6.0$ for myosin, and $A^{1\%}=7.5$ for S1. Purity and quality of proteins were assessed by SDS-polyacryamide gel electrophoresis and ATPase activities. Unless otherwise indicated, all experiments were done in 50 mM KCl, 1 mM $MgCl_2$, 0.2 mM dithiotreitol, and 10 mM Tris-HCl, pH 7.5. S1 concentration was typically 3 μM. The ATP concentration was 2.0 mM.

Steady-State Fluorescence Spectroscopy and Decomposition of Spectra into Log-Normal Components

The steady-state emission spectra were recorded with an SLM-500C specrofluorimeter. Emission was excited at 295 nm. The spectral widths of excitation and emission slits were 4 and 2 nm, respectively. To cancel the effect of fluorescence polarization on the measured value of fluorescence intensity, the polarizer in the excitation path was set at the magic angle (54.7° from the vertical orientation) and polarizer in the emission path was set vertical. The vertical orientation of the emission

polarizer helped to remove Wood's anomalies from the emission monochromator sensitivity curve. Emission spectrum of aqueous solution of L-tryptophan was used as a standard for correction of protein spectra for the instrument spectral sensitivity (21). The intensities of the corrected spectra are proportional to the number of photons emitted per unit wavelength interval. The measurements were carried out at 21°C. The spectra of S1 and S1-ATP complex were measured in the presence of various concentrations of acrylamide. The intensities of fluorescence spectra were corrected for the inner screening effect of acrylamide at the exciting wavelength (31).

The shape of an 'elementary' component of protein fluorescence spectra on the frequency (wavenumber) scale was approximated by uni-parametric log-normal function (21). The resolution into components was performed on sets of spectra measured at various concentrations of quencher (acrylamide) using the SIMS (SImple fitting with Mean-Square criterion) algorithm (20,22). The spectra were independently fitted by one, two or three components. The criterion of attaining the best solution (a sufficient number of components) was the minimal root-mean-square differences (residuals) between theoretical and experimental spectra. For each *i*-th component, the program output data contained the values of spectral maximum position $\lambda_{max}(i)$, the per-cent contribution of the component into the area under total spectrum $S(i)$, Stern-Volmer quenching constant K_{SV} (i) and its ratio to the K_{SV} value for free aqueous tryptophan emission quenching with the same quencher, $K_{rel}(i)$. The maximum position of the total protein fluorescence spectrum was taken from the one-component log-normal description of the spectrum shape. The Stern-Volmer constants K_{SV} (i) were calculated as slopes of the linear plots in coordinates $(A_o/A_c - 1)$ vs. quencher concentration, where A_o and A_c are areas under emission component spectra measured, respectively, in the absence (A_o) and in the presence of quencher in the concentration C (A_c). In order to calculate K_{rel} value, the K_{SV} value for dynamic quenching of free aqueous tryptophan emission with acrylamide was taken to be 16.8 M^{-1} (32,33).

Time-resolved Fluorescence Measurements

Time-resolved fluorescence was measured using a time-correlated single-photon counting (TCSPC) instrument. To avoid a possibility of splitting of all ATP molecules by S1 during the measurements (40 min.) all experiments were carried out at 4°C, and concentrations of S1 and MgATP were 3 μM and 2mM, respectively. The fluorescence was excited by the frequency-doubled output from a cavity-dumped continuous-wave dye laser synchronously pumped by the frequency-doubled output from a mode-locked Nd:YAG laser (Spectra-Physics). Excitation wavelength was tuned to 295 nm. Cavity-dumped dye laser pulses were less than 15 ps wide and followed at a repetition rate of 4,000,000 pulses per second, which made it possible to count up to 20,000 emission photons per second without violating single-photon conditions. Photon counts were stored in 2048 channels, the time window of one channel was 13.33 ps, and overall time resolution of the instrument was 5 channels or 65 ps full-width at half maximum. TCSPC data were collected at 31 emission wavelengths between 300 and 450 nm at 5 nm wavelength step and 8 nm spectral resolution. The data were analyzed globally with the lifetimes being linked across all the emission wavelengths. The results of the global analysis were then renormalized according to the steady-state fluorescence spectrum and represented in the form of decay-associated spectra (DAS). Technical details will be described in a separate paper by Toptygin, Rodgers and Brand.

Analysis of Structural and Physical Parameters of Environment of Tryptophan Residues

The physical and structural parameters of microenvironment of the tryptophan residues in myosin subfragment 1 (X-ray crystal structure of S1 (28); PDB entry 2MYS) was calculated using the original algorithm, which was developed for the analysis of characteristics of environment of tryptophan residues in crystal structures

of proteins in order to compare these characteristics with fluorescence parameters of tryptophan residues (24,26,27). The parameters of microenvironment of each tryptophan residue in S1 were compared with the parameters of microenvironment of tryptophan residues of 18 1-2-3-tryptophan-containing proteins with well identified fluorescence properties (the list of proteins and their PDB-entries presented in Table I), using the statistical method of cluster analysis ("STATISTICA for Windows 5.0" StatSoft, Inc. 1984-1995). We applied tree clustering algorithm and as a distance measure between objects (tryptophan residues) it was used power distance (D):

$$D(x, y) = (\sum_i | x_i - y_i |^p)^{1/r}, \text{ where } p=1, r=4$$

As an amalgamation rule we applied Ward's method that uses an analysis of variance approach to evaluate the distances between clusters (34).

Table I

The list of 18 1-,2-,3-trp proteins applied for cluster analysis.

Cod	Protein name, tryptophan residue	PDB-entry
	1-trp proteins	
AZU	Azurin (*Pseudomonas aeruginosa*), Trp 48	4AZU, 1JOI
PACC	Parvalbumin (cod; Ca-form), Trp 102	Model***
PAM	Parvalbumin (*Gadus merlangus*), Trp 102	1A75
RNT	Ribonuclease T_1 (*Aspergillus oryzae*), Trp 59	9RNT
RCA	Ricin chain A, Trp 211	1RTC
ASP	L-Asparaginase (*E.coli* B), Trp 66	3ECA
VTAH	Viperotoxin, protein A, high ionic strength (*Vipera ammodytes ammodytes*), Trp 30	Model****
GPS	Protein G (*Streptococcus aureus*), Trp 48	1IGD
ASHN	Albumin, serum (human) N-form, Trp 214	1A06, 1BJ5
PLS	Phospholipase A2 (swine pancreas), Trp 3	1P2P, 4P2P
VTB	Viperotoxin, protein B (*Vipera ammodytes ammodytes*), Trp 19	Model****
PLB	Phospholipase A2 (bovine pancreas), Trp 3	2BPP, 1UNE
VTAL	Viperotoxin, protein A, low ionic strength (*Vipera ammodytes ammodytes*), Trp 30	1VPI
GLG	Glucagon, Trp 25	1GCN
	2-trp proteins	
AX6a	Annexin VI (human), Trp 343	1AVC
AX6b	Annexin VI (human), Trp 192	1AVC
A1ATa	α-1-antitrypsin (human), Trp 194	8API, 9API, 2PSI
A1ATb	α-1-antitrypsin (human), Trp 238	8API, 9API, 2PSI
	3-trp proteins	
VTCa	Viperotoxin*, complex Protein A and Protein B (*Vipera ammodytes ammodytes*), Trp 220	1AOK
VTCb	Viperotoxin*, complex Protein A and Protein B (*Vipera ammodytes ammodytes*), Trp 231	1AOK
ENHa	Elastase** (human neutrophyls), Trp 27	1HNE, 1PPF
ENHb	Elastase** (human neutrophyls), Trp 237	1HNE, 1PPF

* Trp 31 in Viperotoxin is practically non-fluorescent, since the probabilities of energy transfer from it to Trp 220 and Trp 231 are 26.2% and 61.6%, respectively.

** Trp 141 in Elastase seems to be non-fluorescent, since its fluorescence is quenched by Nd1 and Ne2 atoms of His 40 and S atom of Met 30, which are located at 4.1Å, 3.9Å, 4.7Å, respectively, from indolic ring.

*** The 3D model was kindly given to us by Drs M. Laberge and J. Vanderkooi.

**** The 3D models was kindly given to us by Dr. B.P. Atanasov.

The fluorescence spectral maxima of S1 and S1-ATP complex were at 336.0±0.5 nm and 335.1 ±0.5 nm, respectively (Table II; Figure 1C), which are in a good agreement with data obtained earlier (4, 11, 12, 35). The decomposition of the tryptophan fluorescence spectrum of S1 into log-normal components, gave reproducibly 3 components with the maxima at 318.8±1.3, 331.8±0.9 and 342.5±0.5 nm (Table II; Figure 1C). When ATP was added, the total emission intensity increased by ca. 18% (Figure 1C). The decomposition of fluorescence spectrum of S1-ATP complex gave almost the same three components with changed partial contributions in the total emission (Table II; Figure 1C). The relative changes in the intensities of the short, intermediate and long wavelength components were –21%, +49%, and +20%, which corresponded to –4.4%, 11.0% and 11.4% changes in the total intensity of S1, respectively (Figure 1C). The intermediate and long wavelength components contributed almost equally in the ATP-induced enhancement of fluorescence. The maximum positions of the emission of short and intermediate wavelength components of S1-ATP complex changed very little; the longest-wavelength component blue-shifted from 342.5 nm to 339.2 nm.

Table II

Fluorescence parameters of S1, S1-ATP complex and their log-normal components.

Protein	λ_{max}, nm of total spectrum	Component number, i	λ_{max} (i), nm	S(i), %	K_{rel}, %
S1	336.0±0.5	1	318.8±1.3	20.7±3.0	3.0±0.4
		2	331.8±0.9	23.0±0.5	2.1±1.5
		3	342.5±0.5	56.3±2.5	109.0±1.8
S1-ATP	335.1±0.5	1	317.4±1.8	13.8±3.0	3.4±1.6
		2	330.3±2.4	28.8±5.7	6.6±4.7
		3	339.2±0.5	57.5±8.7	64.8±9.3

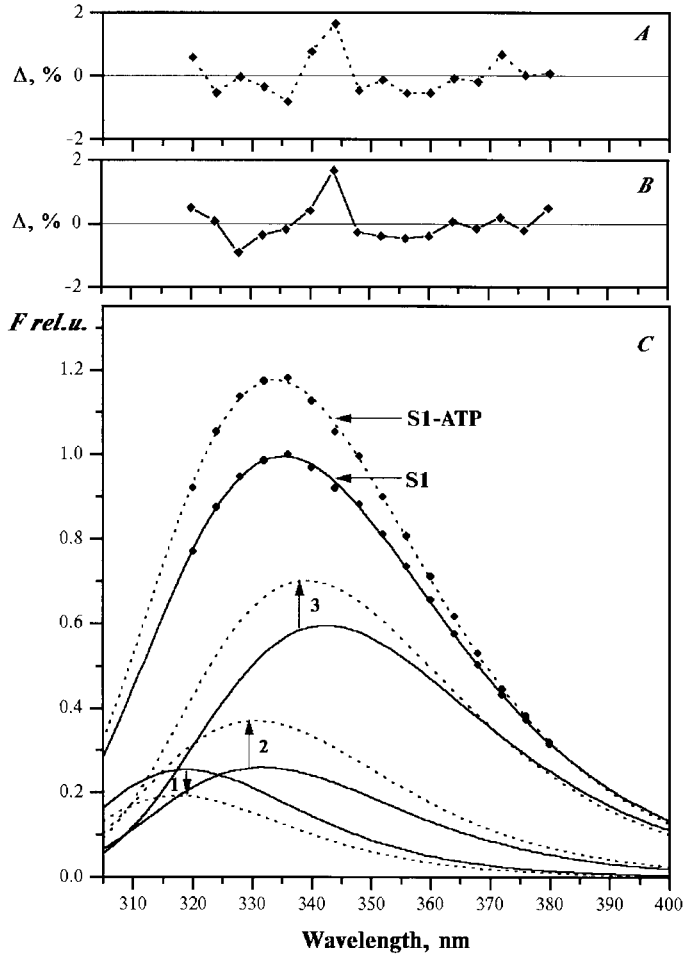

Figure 1: Decomposition of tryptophan fluorescence spectra of S1 and S1-ATP complex into log-normal components. *A, B* – The deviations between theoretical and experimental spectra for S1 (*A*) and S1-ATP complex (*B*) in per cent. *C* – The experimental spectra (circles) and fitting curves (lines) obtained from decomposition of spectra into log-normal components. The spectra of S1 were decomposed into three components (1, 2, 3) in absence (solid lines) and presence (dotted lines) of MgATP. The maxima and relative contributions of components are given in Table I.

Time-resolved fluorescence of S1 and S1-ATP was measured using a time-correlated single-photon counting (TCSDC) method. The data were analyzed globally with lifetimes being linked across all the emission wavelengths (300 – 450 nm). At least three exponentials were required to obtain statically adequate fits to the experimental decay curves. The lifetime values that produced the best fit were: 0.704±0.004, 4.06±0.01, and 9.13±0.02 ns for S1; and 0.713±0.005, 4.03±0.01, and 8.91±0.03 ns for S1-ATP. The decay-associated spectra (DAS) that were calculated from the results of the global fitting and the steady-state emission spectra of S1 and S1-ATP are shown in Figure 2. ATP addition induced negligible changes in the component 1 associated with the shortest lifetime (τ=0.704 ns, λ_{max}=328 nm). The intensity of component 2 associated with the intermediate lifetime (τ=4.06 ns, λ_{max}=333 nm) increased by 9.7% while its peak wavelength remained almost the same (334 nm). The component 3 associated with the longest lifetime (τ=9.13 ns, λ_{max}=345 nm) shifted its peak from 345 to 342 nm and its intensity increased by 10.8%. The time-resolved fluorescence data demonstrated that the ATP-induced fluorescence enhancement was almost equally contributed by the intermediate and long wavelength components in agreement with the results of the decomposition of steady-state fluorescence spectra into log-normal components.

In order to associate the spectral components with the individual tryptophan residues, we carried out the analysis of physical and structural parameters of the microenvironment of tryptophan residues (24,26,27) in the atomic structure of chicken myosin S1 (28) (Figure 3). The set of structural parameters was obtained within the ranges 0-5.5 and 5.5-7.5 Å from each atom of the indole rings of each of five tryptophan residues. The calculated parameters of the microenvironment of indole rings of the tryptophan residues of S1 (Figure 4) are given in Table III. Relative accessibility of Nε1 (*Acc1*) and Cζ2 (*Acc7*) atoms, as well as of the whole indolic fluorophore (*Acc*) of tryptophan residue to water, i.e. the ratio (in per cent) of the accessible surface area of the atoms of indolic ring in protein and in free tryptophan residue in solution, were calculated using Lee and Richards algorithm (36).

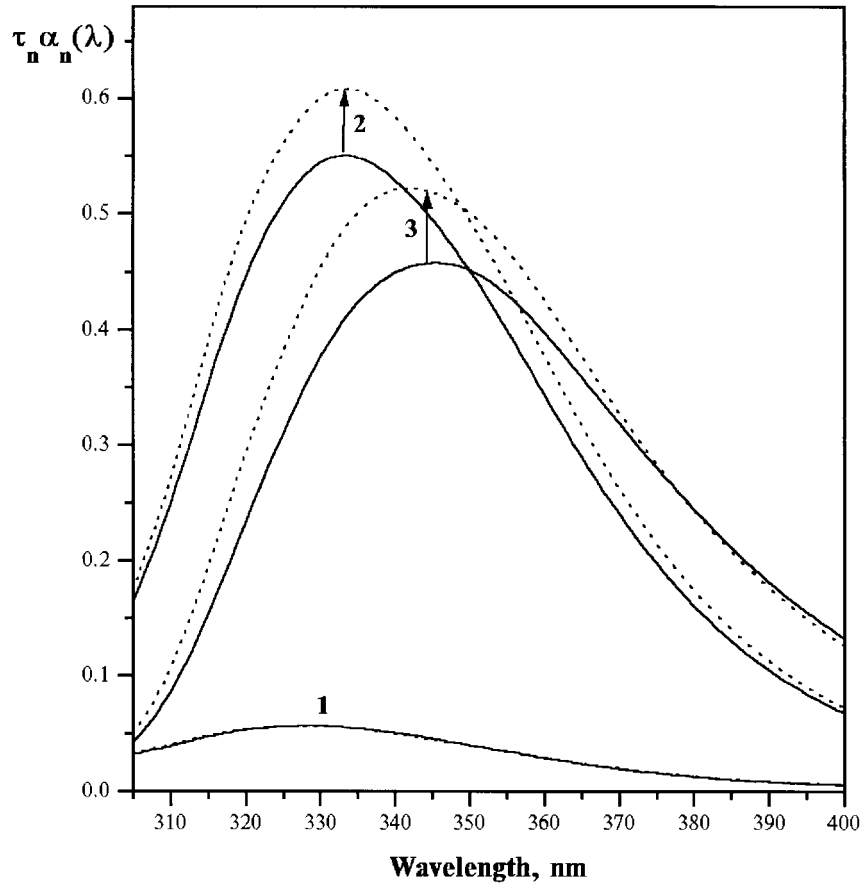

Figure 2: The decay-associated spectra (DAS) corresponding to 4 decay times for S1 (solid lines) and S1-ATP (dashed lines): **1** – 0.7 and 0.71 ns; **2** – 4.06 and 4.03 ns; **3** - 9.13 and 8.91 ns, respectively.

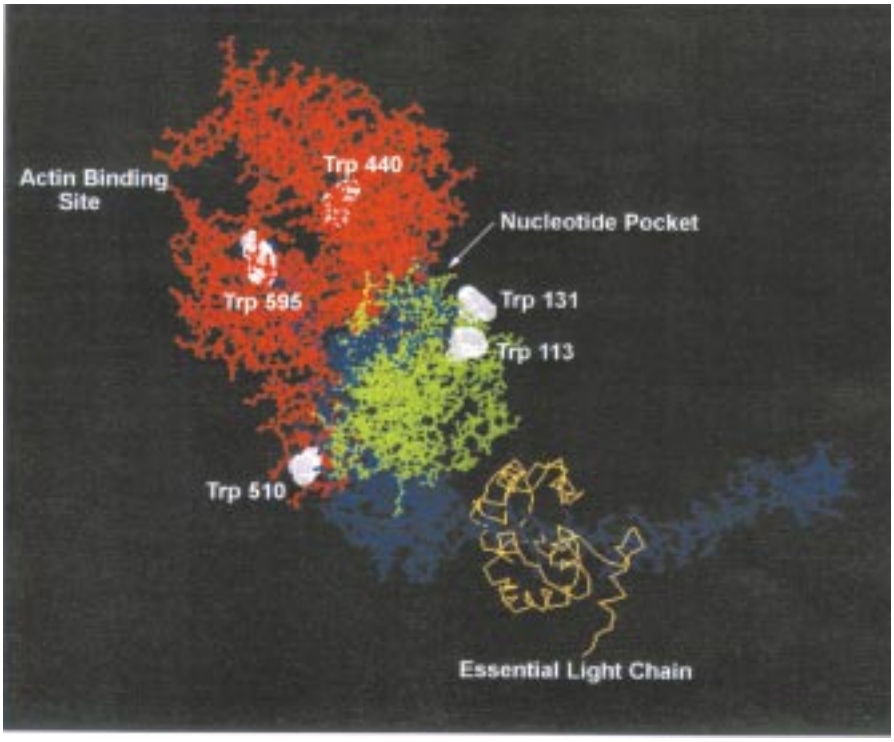

Figure 3: The location of tryptophan residues in skeletal myosin subfragment 1 (PDB entry 2MYS; Rayment et al., 1993). The graphical program is RasMol 2.6

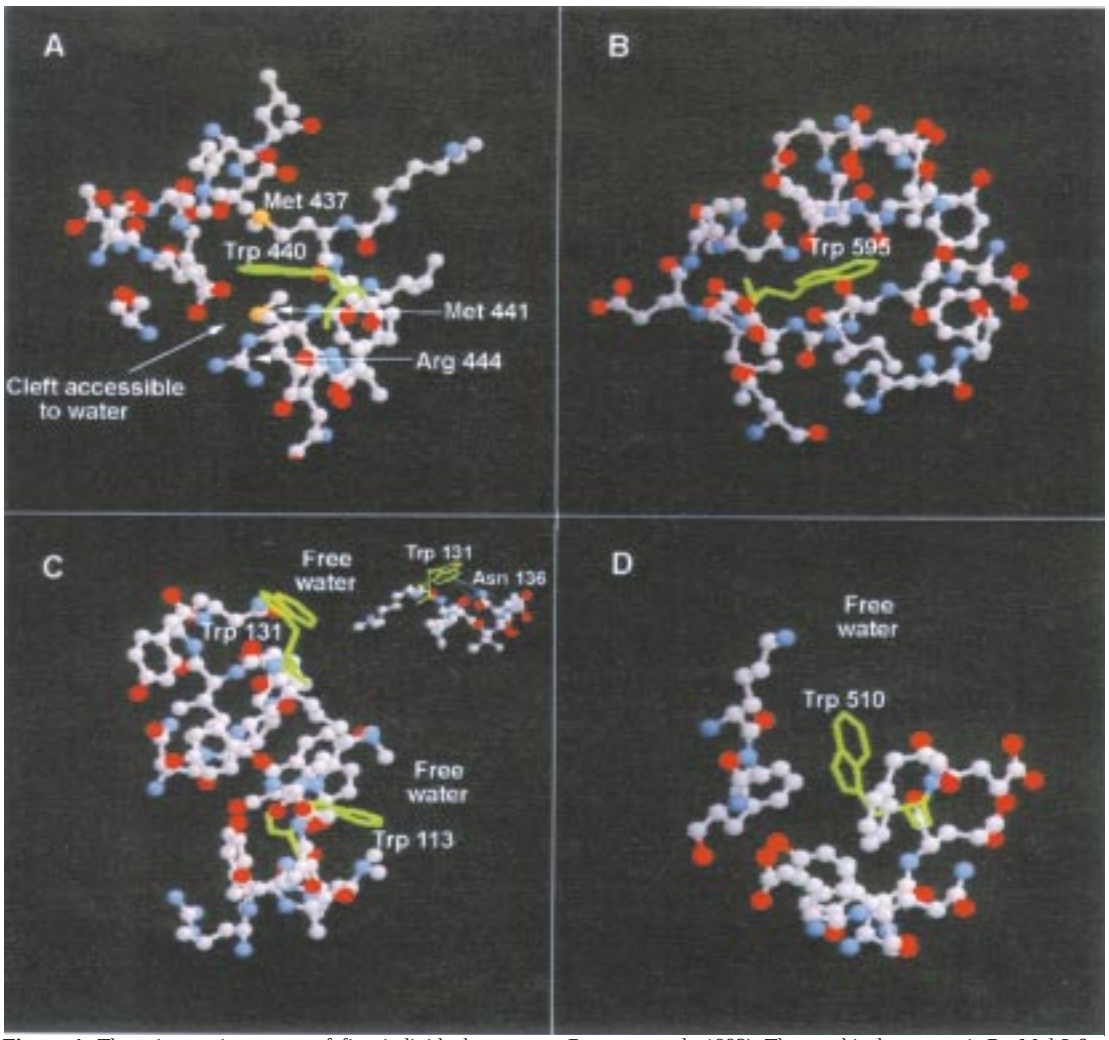

Figure 4: The microenvironments of five individual tryptophan residues of myosin subfragment 1 (PDB entry 2MYS; Rayment et al., 1993). The graphical program is RasMol 2.6

Table III

Physical and structural parameters of microenvironment of 5 tryptophan residues in S1 (PDB-entry 2MYS).

Parameters	Trp113	Trp131	Trp440	Trp510	Trp595
Acc1[1]	0	91.7	41.7	20.8	0
Acc7[2]	35.7	60.7	7.1	46.4	0
Acc[3]	21.8	62.1	9.0	28.6	1.15
Den1[4]	34	23	51	35	67.5
Den2[5]	87	50	122	75	147.5
B1[6]	1.96	2.1	0.99	2.1	1.30
B2[7]	1.89	2.9	1.28	2.3	1.42
D1[8]	42.8	130.5	8.9	60.0	2.29
D2[9]	41.2	180.5	11.6	66.8	2.66
A1[10]	51.4	64.9	27.3	43.7	38.4
A2[11]	39.5	50.3	38.8	33.6	40.7
Fluorescence quenchers:	--	$N\delta_2$ of Asn136 + free water	S Met437 S Met441 $N\varepsilon$, $N\eta_1$,$N\eta_2$ of Arg444	--	--

[1]***Acc1*** - the relative solvent accessibility of Ne1 atom of indolic ring, in per cents;
[2]***Acc7*** - the relative solvent accessibility of Cz2 atom of indolic ring, in per cents;
[3]***Acc*** - the relative solvent accessibility of indolic ring, in per cents;
[4]***Den1*** - packing density (the number of protein and structure water atoms) within the range from 0 to 5.5Å from indolic atoms;
[5]***Den2*** - packing density (the number of protein and structure water atoms) within the range from 0 to 7.5Å from indolic atoms;
[6]***B1*** - relative temperature factor of polar atoms (in relation to the mean value for all Ca atoms) within the range from 0 to 5.5Å from indolic atoms;
[7]***B2*** - relative temperature factor of polar atoms (in relation to the mean value for all Ca atoms) within the layer from 5.5Å to 7.5Å from indolic atoms;
[8]***D1*** = ***Accw.B1*** - parameter, characterizes "dynamic accessibility" within the range from 0 to 5.5Å;
[9]***D2*** = ***Accw.B2*** - parameter, characterizes "dynamic accessibility" within the layer from 5.5Å to 7.5Å;
[10]***A1*** = ***S1*** + (***Accw.S1***)/100, where ***S1*** is a share of polar neighbor polar atoms within the range from 0 to 5.5Å from indolic atoms;
[11]***A2*** = ***S2*** + (***Accw.S2***)/100, where ***S2*** is a share of polar neighbor polar atoms within the layer from 5.5Å to 7.5Å from indolic atoms.

Recent quantum mechanical studies showed that much electron density is lost from Nε1 (Cγ) atoms and deposited at Cζ2 (Cε3, Cδ2) atoms of indole ring during excitation in main fluorescent $^1L_\alpha$ state (37), therefore the interaction of these atoms with highly mobile water molecules should lead to shift of the maximum position of fluorescence spectrum. The packing density (*Den1*, *Den2*), i.e. the number of all heavy (non-hydrogen) protein atoms within the defined space around indole ring, reflects the degree of burying of fluorophore into protein matrix and/or the presence of empty crevices in the structure. The long-wavelength fluorescence spectral shift due to dipole relaxation in surrounding dielectric critically depends on the ratio of the relaxation time to the fluorescence lifetime of a fluorophore. The relaxation of the large dipoles of bulk water molecules could be very fast (a few hundreds of femtoseconds), while the relaxation of dipoles of protein groups may be longer than several nanosecond of emission lifetime (37). Therefore, it was estimated parameters, which reflect a mobility of polar groups around fluorophores. Protein crystallography provides such a parameter as atomic temperature factor (Debye-Waller factor or B-factor (38)). We calculated the temperature B-factors of polar atoms normalized to the mean value of all Cα atoms in crystal structure in both near (*B1*) and far (*B2*) layers from indole atoms. To account for a common effect of both mobility of neighbor polar atoms and the accessibility of indole ring to free highly mobile water it was calculated the parameters of "dynamic accessibility" (*R1, R2*). The last two parameters (*A1* and *A2*) may be considered as a polar-

ity measure of the microenvironment of an indole ring assessed by the number of polar groups within the above defined distance ranges.

Fluorescence of tryptophan residues might be partially or totally quenched by some neighbor protein groups (33,39-44) or due to energy homo-transfer to another indole chromophore (45-48). The calculated probabilities of excitation energy transfer (using parameters taken from 49-50) within all pairs of tryptophan residues of S1 did not exceed 1%, which allowed us to consider the emission spectrum of S1 as a simple sum of contributions of 5 fluorophores. A detailed analysis of the distances and orientations of the side chains of all polar groups around 5 indole rings in S1 allowed us to reveal a possible quenching groups of tryptophan fluorescence (see Table III, last row).

The assignments of spectral emission components to individual tryptophan residues in S1 was carried out using the principle according which the more accessible residue has to possess emission at longer wavelengths. (24-27,40,51-53). Also the parameters of microenvironment of 5 tryptophan residues of S1 were compared with the same physical and structural characteristics of 1-2-3-tryptophan-containing proteins with well known fluorescence properties applying cluster analysis method. This method has been successfully applied to classification problems in different fields of science, in particular, for the classification of various structural parameters of proteins (54-57). The purpose of the joining (tree clustering) algorithm applied here, is to join objects (i.e., tryptophan residues) into clusters (groups) with similar parameters. The results of cluster analysis are presented as a hierarchical tree diagram (dendrogram) (Figure 5). It was revealed 3 major groups (A, B and C).

Group C consist of long-wavelength emitting protein tryptophans. Among these tryptophan residues are fluorophores of single-tryptophan containing proteins, such as glucagon, porcine and bovine pancreatic phospholipases A_2, viperotoxin protein B (*Vipera ammodytes ammodytes*), and streptococcal protein G, which emit with spectral maxima at 340-345 nm (58-61). The results of cluster analysis demonstrate that Trp113, 131 and 510 belong to the group C (Figure 5). These tryptophans are well exposed to the solvent and their protein environment is rather mobile (Table III; Figure 4C, D). Therefore, we can associate the longest-wavelength and longest-

Figure 5: Dendrogram constracted based on the parameters of microenvironment of 22 tryptophan residues of 18 1-2-3-tryptophan containing proteins (Table III) and 5 tryptophan residues of S1 (27 tryptophan residues). Amalgamation rule is a Ward's method, Distance measure is a power distance $(\sum|x-y|)^{1/4}$. Program package STATISTICA 5.0.

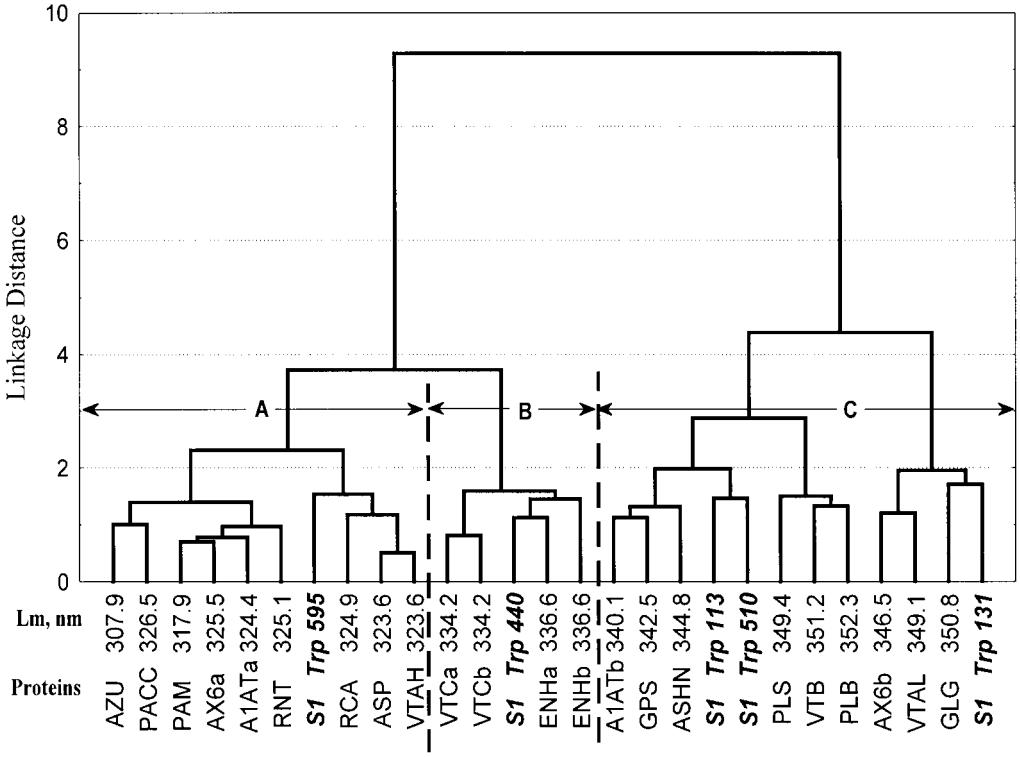

lifetime component (τ~ 9.0 ns, λ_{max} ~ 341 nm and high quencher accessibility, K_{rel}, Table II) of S1 with Trp113, 131 and 510. The Trp131, which is very mobile (*B1*=2.1 and *B2*=2.9), is completely accessible to water molecules (the highest accessibilities and high *R1, R2* values and the lowest value of packing density, see Table III). Near to Trp131 (4-5Å) there is located the water accessible amide group of Asn136 (Figure 4C). Its Nδ2 and Oδ1 atoms are turned towards the Cζ2 and Cη2 atoms of Trp131. Much electron density could be localized on the Cζ2 atom of indolic ring during excitation (37). As a result, the amide group of Asn136 may form together with water molecules an electron trap (47), which might at least partially quench the Trp131 emission.

The other two tryptophan residues, Trp440 and Trp595, are buried in the protein interior (Figure 3). Trp595 is located in hydrophobic environment (Table III; Figure 4B). The solvent accessibilities for all indolic atoms of Trp595 are equal to zero. The values of packing density around Trp595 are very high: Trp595 belongs to group A that consist of single-tryptophan-containing proteins such as *E. coli B* L-asparaginase, cod parvalbumin and RNase T1, which possess fluorescence spectra with maxima at 316-325 nm, (50,62-68). Therefore, we assume that the component of S1 fluorescence spectrum with λ_{max} of ca. 318 nm should be assigned to Trp595. It is likely that Trp595 has a shortest fluorescence lifetime.

Trp440 is located in a more polar environment than Trp595. It is a little exposed to the solvent (*Acc*=9.0%; Table III; Figure 4A). Its packing densities have intermediate values. Trp440 falls in group B of the dendrogram where are located tryptophan residues emitting with maximum at 330-335 nm (25,27). Therefore, the intermediate component λ_{max} of ca. 331 nm, τ = 4.02 ns) can be assigned to Trp440.

Discussion

We used two different approaches to decompose the fluorescence spectra of S1 into components associated with the individual tryptophans or groups of tryptophans. The decomposition of steady-state spectra into log-normal components allows us to reveal the groups of tryptophans according to the positions of their spectral maxima. Siano and Metzler (69) have showed that the absorption spectra of organic molecules could be described by four-parametric log-normal functions (asymmetric Gaussian function). Later, it was demonstrated that fluorescence spectra of many organic molecules, including tryptophan, its derivatives and tryptophan residues in proteins could be accurately described on the frequency scale by log-normal function but in its mirror-symmetric form (21,47). Due to the linear relationship between the positions of spectral maxima and the two half-maximal amplitudes for tryptophan derivatives in various solvents, the shape of tryptophan fluorescence spectrum is entirely determined by the position of spectral maximum of their emission spectra (21). This fact allowed the development of stable algorithms for resolution of composite fluorescence spectra of proteins into log-normal components (20-22). This method enabled us to reveal three emitting groups of tryptophans in S1 with λ_{max} at ca. 318, 331, and 342 nm. These components are very much similar to the decay-associated spectra obtained in this work (Figure 2) and by Torgerson (11). Both methods demonstrated that there are two groups of ATP-sensitive tryptophans with emission maxima at ca. 331 and 342 nm.

The structural parameters shown in Table III and the cluster dendrogram (Figure 5) indicate that Trp113, 131 and 510 in S1 are exposed to the solvent, while Trp595 and 440 are buried in protein. Trp595 is in hydrophobic environment and should emit at very short wavelength. This tryptophan determines likely the shortest wavelength component ($\lambda_{max} \approx$ 318 nm). This component is much weaker than other two components and less sensitive to the effect of ATP. Therefore Trp595 could not be responsible for ATP-induced fluorescence increase. ATP induced an increase in intensities of intermediate (331 nm, 4.02 ns) and long wavelength (341 nm, 9.0 ns)

components, and these two components contributed almost equally to the total enhancement of fluorescence. The exposed tryptophans contribute to the long wavelength component with $\lambda_{max} \approx 340$ nm and t = 9.0 ns. Upon binding of ATP to S1 this component was blue shifted by 3 nm, and its intensity increased. The blue shift indicates that some of the exposed tryptophan residues may move to a more hydrophobic and/or more rigid environment in presence of ATP. It seems that Trp510, which is exposed to solvent in the absence of ATP, may be partially buried into the protein interior in the presence of ATP (16, 17, 70). Trp440 most likely contributes in the intermediate wavelength component (ca. 331 nm). Since the lifetime for this component is not changed, we assume that ATP may decrease the degree of static quenching of Trp440 emission by some of the vicinal amino acid residues (Met437, Met441 and/or Arg444) and increase its fluorescence intensity. It is likely that Trp510 and Trp440 are the main contributors to fluorescence enhancement of skeletal S1 by ATP. Contributions of these tryptophans may vary in different myosins. Comparison of the structures of chicken skeletal, *Dictyostelium* and smooth muscle S1 showed that in the microenvironment of tryptophans corresponding to chicken Trp440 the residues Met437 and Met441 are replaced by Leu429 and Leu433 in Dicty S1, and by Leu438 and Ile442 in smooth S1. The lack of methionine quenching groups would result in the lower sensitivity of Trp432 (Dicty S1) and Trp441 (smooth S1) to the ATP binding. Indeed, it has been shown recently that Trp501 of Dicty S1 is mainly responsible for the ATP-induced enhancement of fluorescence (18). The microenvironment of tryptophan residues corresponding to Trp510 of chicken skeletal S1 is more conserved in myosins, and these tryptophans might be sensitive to ATP in all myosins.

Trp440 is included in the long α-helix (419-449) located in the upper subdomain of central fragment of S1 (Figure 3). This a-helix is stretched from actin binding site, segment 405-415, to the ATP binding site, segment 462-474 (Switch II), and may play a role in the communication between these two sites. On the other hand the segment 462-474 is connected via α-helix 475-505 to the loop containing Trp510. The α-helix 475-505 might be involved in the transduction of structural changes in ATP-binding center to the S1 tail.

Acknowledgments

The authors are cordially thankful to Dr Boris P. Atanasov (Institute of Organic Chemistry, Bulgarian Academy of Sciences, Sofia, Bulgaria) for 3D models of viperotoxin subunits and to Drs Monique Laberge and Jane Vanderkooi (University of Pennsylvania, Philadelphia, PA) for the 3D model of cod parvalbumin. The work was supported by the grants: Russia Foundation for Basic Researches #97-04-49449 and 00-04-48127 (E.B. & Ya.R.); IUMBMB Wood/Whelan Fellowship (Ya.R.) and NIH grant AR40095-06 (J.B. & O.A.).

References and Footnotes

1. F. Morita, *J. Biol. Chem. 242*, 4501-4506 (1967).
2. E.A. Burstein, *Abh. Deutschen Akad. Wiss. Berlin, Klasse Med. 4*, 243-249 (1966).
3. E.A. Burstein. *J. Appl. Spectrosc. (Minsk) 5*, 81-84 (1967) [in Russian].
4. M. M. Werber, A.G. Szent-Gyorgyi and G.D. Fasman, *Biochemistry 11*, 2872-2883 (1972).
5. O.A. Andreev, S.N. Udaltsov, Z.E. Rogdestvenskaya and V.V. Lednev, *Studia Biophys. 134*, 249-256 (1989).
6. S. Papp, D. Eden and S. Higsmith, *Biochim. Biophys. Acta 1159*, 267-273 (1992).
7. C.R. Bagshaw and D.R. Trentham, *Biochem. J.* 141, 331-349 (1974).
8. S.P. Chock and E. Eisenberg, *J. Biol. Chem. 254*, 3229-3235 (1979).
9. K.M. Trybus and E.W. Taylor, *Biochemistry 21*, 1284-1294 (1982).
10. J.M. Chalovich, L.A. Stein, L.E. Greene and E. Eisenberg, *Biochemistry 23*, 4885-4889 (1984).
11. P.M. Torgerson, *Biochemistry 23*, 3002-3007 (1984).
12. M.M. Werber, Y.M. Peyser and A. Muhlrad, *Biochemistry 20*, 2903-2909 (1987).
13. Y.M. Peyser, A. Muhlrad and M.M. Werber, *FEBS Lett. 259*, 346-348 (1990).
14. W.C. Johnson, D.B. Bivin, K. Ue and M.F. Morales, *Proc. Natl. Acad. Sci. U.S.A. 88*, 9748-9750 (1991).

15. T. Hiratsuka, *J. Biol. Chem. 267*, 14949-14954 (1992).
16. S. Park, K. Ajtai and T.P. Burghardt, *Biochim. Biophys. Acta 1296*, 1-4 (1996).
17. S. Park, K. Ajtai and T.P. Burghardt, *Biophys. Chem. 63*, 67-80 (1996).
18. R. Batra and D.J. Manstein, *Biol. Chem. 380*, 1017-1023 (1999).
19. M.D. Ritchie, M.A. Geeves, S.K.A. Woodward and D.J. Manstein, *Proc. Natl. Acad. Sci. U.S.A. 90*, 8619-8623 (1993).
20. S.M. Abornev and E.A. Burstein, *Molecular Biology (Moscow) 26*, 890-897, 1992 [Engl. translation].
21. E.A. Burstein and V.I. Emelyanenko, *Photochem. Photobiol. 64*, 316-320 (1996).
22. E.A. Burstein, S.M. Abornev and Ya.K. Reshetnyak, *Biophys. J.* (submitted).
23. J.R. Knutson, D. Walbridge and L. Brand, *Biochemistry 21*, 4671-4679 (1982).
24. Ya. K. Reshetnyak and E.A. Burstein, *Biophysics (Moscow) 42*, 267-274 (1997) [Engl. translation] .
25. E.A. Burstein and Ya.K. Reshetnyak, *Biophys. J. 74*, A181 (1998).
26. Ya.K. Reshetnyak, *Ph.D. thesis*, ITEB RAN, Pushichino, Russia (2000) [In Russian].
27. Ya.K. Reshetnyak, Yu. Koshevnik and E.A. Burstein, *Biophys. J.* (submitted).
28. I. Rayment, W. Rypniewski, K. Schmidt-Base, R. Smith, D.R. Tomchik, M.M. Benning, D.A. Winkelman, G. Wesenberg and H.M. Holden, *Science 261*, 50-58 (1993).
29. Y. Tonomura, P. Appel and M.F. Morales, *Biochemistry 5*, 515-521 (1996).
30. A.G. Weeds and R.S. Taylor, *Nature 257*, 54-56 (1975).
31. E.A. Burstein, *Biophysics (Moscow) 13*, 433-442 (1968) [in Russian].
32. T.G. Bukolova-Orlova, E.A. Burstein and L.Ya. Yukelson, *Biochim. Biophys. Acta. 342*, 275-280 (1974).
33. T.L. Bushueva, E.P. Busel, V.N. Bushuev and E.A. Burstein, *Studia Biophys. 44*, 129-132 (1974).
34. J.H. Ward, *J. Am. Stat. Assoc. 58*, 236 (1963).
35. D.I. Levitsky, N.V. Khvorov, V.L. Shnyrov, N.S. Vedenkina, E.A. Permyakov and B.F. Poglazov, *FEBS Lett. 264*, 176-178 (1990).
36. B. Lee and F.M. Richards, *J. Mol. Biol. 55*, 379-400 (1971).
37. P.R. Callis, *Meth. Enzymol. 278*, 113-150 (1997).
38. H. Frauenfelder, G.A. Petsko and P. Tsernoglou, *Nature 280*, 558-568 (1979).
39. R.W. Cowgill, *Biochim. Biophys. Acta. 207*, 556-559 (1970).
40. N.G. Bakhshiev, *Spectroscopy of Intermolecular Interactions.* Nauka, Leningrad (1972) [In Russian].
41. T.L. Bushueva, E.P. Busel and E.A. Burstein, *Studia Biophys. 52*, 41-52 (1975).
42. K. Willaert and Y. Engelborghs, *Eur. Biophys. J. 20*, 177-182 (1991).
43. Y. Chen and M.D. Barkley, *Biochemistry 37*, 9976-9982 (1998).
44. T. Yuan, A.M. Weljie and H.J. Vogel, *Biochemistry 37*, 3187-3195 (1998).
45. S.V. Konev, *Fluorescence and Phosphirescence of Proteins and Nucleic Acids*. Plenum Press, New York (1967).
46. I.Z. Steinberg, *Ann. Rev. Biochem. 40*, 83-114 (1971).
47. E.A. Burstein, Luminescence of Protein Chromophores: The Model Studies in *Adv. Sci. & Eng. (Ser. Biophysics) vol. 6*, VINITI, Moscow (1976) [in Russian].
48. R.E. Dale and J. Eisinger, *Biopolymers 13*, 1573-1605 (1974).
49. J. Eisinger, B. Feuer and A. A. Lamola, *Biochemistry 8*, 3908-3915 (1969).
50. Y. Yamamoto and J. Tanaka, *Biochim. Biophys. Acta. 207*, 522-531 (1970).
51. E.A. Burstein, N.S. Vedenkina and M.N. Ivkova, *Photochem. Photobiol. 18*, 263-279 (1973).
52. Ya.K.Reshetnyak and E.A. Burstein, *Biophysics (Moscow) 42*, 785-795 (1997) [Engl. translation].
53. J.R. Lakowicz, *Principles of Fluorescence Spectroscopy*. Plenum Press, New York (1983).
54. N.S. Boutonnet, M.J. Rooman and S.J. Wodak, *J. Mol. Biol. 253*, 633-647 (1995).
55. K.F. Han, C. Bystroff and D. Baker, *Protein Sci. 6*, 1587-1590 (1997).
56. P.C. Sanschagrin and L.A. Kuhn, *Protein Sci. 7*, 2054-2064 (1998).
57. F. Drablos, *Bioinformatics 15*, 501-509 (1999).
58. B.P. Tchorbanov, B.V. Alexiev, T.G. Bukolova, E.A. Burstein and B.P. Atanasov, *FEBS Lett. 76*, 266-268 (1977).
59. T.G. Bukolova-Orlova, N.Y. Orlov, E.A. Burstein, B.P. Tchorbanov and B.V. Alexiev, *Arch. Biochem. Biophys. 200*, 216-222 (1980).
60. M.R. Eftink and K.A. Hagaman, *Biophys. Chem. 25*, 277-282 (1986).
61. E.A. Permyakov and G.Y. Deikus, *Molecular Biology (Moscow) 29*, 159-167 (1995) [In Russian].
62. S. Shifrin, S.W. Luborsky and B.J. Grochowski, *J. Biol. Chem. 246*, 7708-7714 (1971).
63. R.B. Homer, *Biochim. Biophys. Acta 278*, 395-398 (1972).
64. E.A. Burstein, Intrinsic Protein Luminescence: Nature and Applications in *Adv. Sci. & Eng. (Ser. Biophysics) vol. 7*, VINITI, Moscow (1977) [in Russian].
65. M.R. Eftink, *Meth. Biochem Analysis 35*, 127-205 (1991).
66. E.A. Permyakov, V.V. Yarmolenko, E.A. Burstein and Ch. Gerday, *Biophys. Chem. 15*, 19-26 q (1982).
67. J.W. Longworth, *Photochem. Photobiol. 7*, 587-596 (1968).
68. V.M. Grishchenko, V.I. Emelyanenko, M.N. Ivkova, S.I. Bezborodova and E.A. Burstein, *Bioorgan. Chem. (Moscow) 2*, 207-216 (1976) [In Russian].

69. D.B. Siano and D.E. Metzler, *J. Chem. Phys. 51*, 1856-1861 (1969).
70. K. Ajtai and T.P. Burghardt, *Biochemistry 34*, 15943-15952 (1995).

Date Reveived: April 16, 2000

Communicated by the Editor Valery Ivanov